On the use of CO_2 laser induced surface patterns to modify the wettability of Poly(methyl methacrylate) (PMMA)

David Garreth Waugh and Jonathan Lawrence

Wolfson School of Mechanical and Manufacturing Engineering, Loughborough University, Leicestershire, LE11 3TU, UK

Corresponding author:

David Waugh
Wolfson School of Mechanical and Manufacturing Engineering
Loughborough University
Loughborough
LE11 3TU, UK
Email: D.G.Waugh@lboro.ac.uk

Tel: 01509 227593

Fax: 01509 227648

1.0 – Abstract

CO_2 lasers can be seen to lend themselves to materials processing applications and have been used extensively in both research and industry. This work investigated the surface modification of PMMA with a CO_2 laser in order to vary the wettability characteristics. The wettability characteristics of the PMMA were modified by generating a number of patterns of various topography on the surface using the CO_2 laser. These induced patterns were trench and hatch with scan dimensions of 50 and 100 μm. Through white light interferometry it was found that for all laser patterned samples the surface roughness had significantly increased by up to 3.1 μm. The chemical composition of selected samples were explored using X-ray photoelectron spectroscopy and found that the surface oxygen content had risen by approximately 4% At. By using a sessile drop device it was found that, in comparison to the as-received sample, 50 μm dimensions gave rise to a more hydrophilic surface; whereas 100 μm dimensions gave rise to either no change in contact angle or an increase making the PMMA hydrophobic. This can be explained by combinations of surface roughness and γ^p contributing to the observed contact angle, in addition to the possibility of different wetting regimes taking place owed to the variation of topographies over the as-received and laser patterned samples.

Keywords: CO_2 laser, PMMA, Wettability, Surface modification.

2.0 – Introduction

Over the past 10 years it has been shown that polymers have the potential to be used in a number of applications such as biomedical [1-4] and MEMS/NEMS [5]. In general, it is seen that most polymer materials possess poor adhesion characteristics and, as a direct result of this, tend to be difficult to wet, having inferior bond qualities [6]. Numerous researchers have endeavored to surface modify the surface of polymers to improve upon the adhesion and wettability characteristics. This has especially been seen throughout biomedical applications in which polymeric biomaterials have adequate bulk properties but lack sufficient surface properties in terms of efficient cell response [4,7]. From this, it can be seen that it is crucial for polymers that the surfaces are modified in order to enhance the consequent intended use. For instance it was discussed by Milde et al. [8] that, owed to the inert nature of polymer surfaces, numerous plastics are unable to be coated with sufficient adhesion highlighting the need for these plastics to have pretreatment prior to the application. In addition to this, Riyadh et al. [9] found that surface modification of polyimide could give rise to improved adhesion characteristics for a thin metal coating which, when applied to space applications, can reduce the adhesion for unwanted contaminants. Furthermore, in

consideration of wettability and bioactive cell response a number of experiments have been carried out which has identified that the both of these parameters can be enhanced and modified by means of laser surface patterning [10-13].

A number of techniques have been implemented to achieve surface modifications such as surface coatings [14], plasma [15] and lithography [16,17]. These techniques offer a number of advantages but can be costly, require high maintenance and also require high user involvement. An alternative method offering flexibility, accuracy and negligible bulk modification is that of laser surface patterning. Utilizing lasers in this manner can be seen to a very attractive method for varying surface properties as they also allow for relatively clean processing emphasizing the reduced need for post-processing. In terms of laser beam interactions with materials, the way a material responds to the incident laser is highly dependant upon a number of parameters. Specific to polymers, IR lasers give rise to resonant coupling in the form of bond and lattice vibrations allowing for the processing to be thermolytical. This is due to the fact that the photon is only weakly absorbed by the polymer, with the energy that has been absorbed being distributed to vibrational modes [18]. With most lasers it is seen that the smallest possible features that can be achieved are on the micron scale; however, nano-structures have been achieved using a laser emitting at a wavelength of 157 nm [19].

The study of wettability has been a major focal point for many researchers and has been applied to a wide range of applications such as biomedical [15,20,21], coating technologies [22,23] and adhesion [5,24,25]. As the interface between a solid and liquid can be very complex it is necessary to account for the wetting regime that takes place. Two of the most common wetting regimes is that of Wenzel and Cassie-Baxter. The Wenzel regime describes a liquid which, when in contact with a surface, completely wets the surface [26,27]; whereas the Cassie-Baxter regime is applied to those systems which give rise to the formation of air pockets along the liquid-solid interface [28-30]. However, in some cases it has been seen that it may be possible for a hydrophilic surface to give rise to some form hybrid wetting regime owed to the roughness and topographical pattern on the surface [31,32]. In this instance, it is seen in some cases that upon increasing the surface roughness, through the patterning of a surface, the contact angle can increase. On another note it has also been observed that in general, when the surface energy and it's components are a dominant factor, the contact angle is an inverse function of the polar component of the surface [4].

Leading on from this, it can be seen that it would be advantageous to devise a repeatable technique which would allow material surfaces to be modified in order to optimize that surface for the required application. As lasers offer an attractive means of allowing surfaces to be modified topographically and chemically, with negligible effect to the bulk properties, this paper details how the wettability of PMMA

in terms of the recently advancing contact angle can be modified by implementing CO_2 laser induced patterns.

3.0 – Experimental Procedure

3.1 – Laser Irradiation Procedure

The PMMA was sourced in 150×150 mm sheets with a thickness of 5 mm (Goodfellow Cambridge, Ltd). A 1kW continuous wave (cw) CO_2 laser (Everlase S48; Coherent, Ltd) was used to obtain a conveniently sized PMMA sample for experimentation. That is, the as-received PMMA sheet was cut into 30 mm diameter discs. No discernible heat affected zone (HAZ) was observed under optical microscopic examination.

In order to generate the required marking pattern with the 10.6 μm Synrad cw 10W CO_2 laser system Synrad Winmark software version 2.1.0, build 3468 was used. In addition, the software was capable of using images saved as .dxf files which can be produced by using CAD programs such as, in this case, Licom AutoCaM. The PMMA samples where placed into the laser system onto a stage and where held in place using a bracket with a 30.5 mm diameter hole cut into the centre of the bracket. The surface of the sample was placed at the focus of the laser system which was 250 mm away from the output facet of the laser system. To achieve the required pattern the system utilized a galvanometer scanner to scan the 95 μm spot size beam directly across the stationary target material. It should be noted that the target material and laser system was held in a laser safety cabinet in which the ambient gas was air and an extraction system was used to remove any fumes produced during laser processing.

In all instances, to induce the intended surface pattern the laser parameters were kept constant with the power set to 70% (7W) and traverse scanning speed being 600 mms^{-1}. 4 samples were laser processed in which the four patterns induced onto the surfaces of the PMMA samples were: trenches with 50 μm spacing (T50), hatch with 50 μm spacing (H50), trenches with 100 μm spacing (T100) and hatch with 100 μm spacing (H100). In addition, an as-received control sample was used (AR). It should also be noted here that the dimensions stated for the laser patterned samples are that of the laser scanning dimensions and not of the resulting laser-induced pattern.

3.2 – Topography, Wettability Characteristics and Surface Chemistry Analysis

After the laser patterning, the PMMA samples were analysed using an optical microscope (Flash 200 Smartscope; OGP, Ltd) to obtain optical micrographs of the samples. Also, surface profiles of the samples were determined using a white light interferometer (WLI) (NewView 500; Zygo, Ltd) with

MetroPro and TalyMap Gold Software. The Zygo WLI was setup using a ×10 Mirau lens with a zoom of ×0.5 and working distance of 7.6 mm. This system also allowed Sa and Ra roughness parameters to be determined for each sample.

In accordance with the procedure detailed by Rance [33] the samples were ultrasonically cleaned in isoproponal (Fisher Scientific Ltd., UK) for 3 minutes at room temperature before using a sessile drop device (OCA20; Dataphysics Instruments, GmbH) to determine various wettability characteristics. This was to allow for a relatively clean surface prior to any contact angle measurements being taken. To ensure that the sample surfaces were dry a specimen dryer (Metaserv, UK) was utilized to blow ambient air across the samples. To obtain recent advancing and receding contact angles using triply distilled water and the recent advancing angles using diodomethane for each sample the sessile drop device was used with relevant software (SCA20; Dataphysics Intrsuments, GmbH). By utilizing the advancing contact angles for the two liquids with the software an Owens, Wendt, Rabel and Kaeble (OWRK) plot was produced to determine the surface energy of the samples. For the two reference liquids the SCA20 software used the Ström et al. technique to calculate the surface energies of the samples. It should be noted here that ten contact angles, using two droplets, in each instance was recorded to achieve a mean contact angle for each liquid and surface.

All samples were sputter coated with Au to attain adequate conductance and analysed using scanning electron microscopy (SEM). In addition, prior to coating for SEM, X-ray photoelectron spectroscopy (XPS) analysis to allow any surface modifications in terms of chemical composition due to the laser irradiation to be revealed.

4.0 – Results and Discussion

4.1 – Effect of Laser Irradiation on Topography

It has been shown previously that CO_2 lasers, such as the Synrad system used in this instance, possess the ability to significantly surface modify polymers [34]. Throughout this study it has been seen that laser surface modification of PMMA, through employing the Synrad cw CO_2 laser, is no exception. For instance, it is evident from the micrographs shown in Figure 1 that the laser induced patterns (see Figures 1(b) – 1(e)) gave rise to considerable melting of the surface. This arises due to the fact that the 10.6 μm laser beam interaction with the PMMA surface is a thermolytical process owed to the laser coupling into the material in the form of bond and lattice vibrations. Figure 1 also highlights, qualitatively, the major differences between induced surface patterns as well as between the as-received sample. It can be seen that the trench and hatch patterns with 50 μm spacing (see Figures 1(b) and (d)) gave rise to considerably more melting in comparison to that of the trench and hatch patterns with 100 μm

spacing (see Figures 1(c) and (e)). This was a result of the spot size of the laser beam at the surface of the material was 95 μm which gave rise to the pattern overlapping on the 50 μm spaced samples, causing areas to re-melt and re-solidify. It is also necessary to note here that the hatch patterns (H50 and H100) shown in Figure 1(d) and (e) appear to have had the topographical hatch more prominent in the y-axis in comparison to the x-axis. This is on account of the way in which the laser interacted with the material as the laser scanned the pattern across the material surface. In order to confirm what was observed through optical microscopic analysis the samples were also studied by obtaining SEM images which can be seen in Figure 2.

Like the optical microscopy analysis, SEM analysis of the samples (see Figure 2) showed that the surface of the laser patterned PMMA samples had been amply modified in comparison to that of the as-received sample. It was also interesting to see that SEM images of the 50 μm spaced patterns (see Figures 2 (b) and (d)) indicated that the intended topographical pattern had been slightly distorted due to the large amount of surface melting that appears to have taken place. Furthermore, from Figure 2 (d) it was suggested that the 50 μm hatch pattern (H50) gave rise to a smoother surface in comparison to the other laser patterned samples which can be accounted to the surface melting and re-melting. Whereas SEM images of the other laser patterned samples (see Figure 2 (a) – (c) and (e)) imply that, owed to the surface melting and re-solidifying, protrusions away from the surface formed resulting in a considerable increase in surface roughness.

In order to obtain the roughness parameters quantatively, WLI was employed which allowed for continuous axonometric images and surface profile extractions to be generated. This allowed a 3-D profile of each of the sample surfaces to be obtained. Figure 3 shows the continuous axonometric image with corresponding profile extraction for the as-received reference sample. The continuous axonometric and profile extraction for the as-received sample shown in Figure 3 revealed that in relation to the laser patterned samples the surface of the as-received sample (AR) was markedly smoother with peak heights of up to 0.4 μm leading to Sa and Ra values of 0.04 and 0.03 μm, respectively. This is contrasted with the laser patterned samples, in which the continuous axonometric images and profile extractions for the laser patterned samples can be seen in Figure 4 – 7. Figure 4 shows the resulting continuous axonometric and profile extraction from the WLI analysis of the 50 μm trench patterned sample. From this, it can be seen that the surface topography for the 50 μm trench sample is considerably rougher in comparison to the as-received sample with peak heights of up to 10 μm and roughness values of 2.66 and 1.63 μm for Sa and Ra, respectively. Similar values with an Sa of 2.65 μm, an Ra of 1.43 μm and peak heights ranging between 10 and 15 μm, were also observed for the sample laser patterned using 100 μm trenches (see Figure 5). It is evident from both Figures 4 and 5 that a significant amount of surface melting has taken

place as a direct result of the laser-material interaction. This melting and re-solidification can be seen to eliminate some of the intended periodic pattern induced by the laser processing. This can also be seen in Figures 6 and 7 which depict the results from the WLI analysis of the 50 and 100 μm hatch patterns, respectively. The elimination of the intended periodic pattern is highly demonstrated with the observed results of the 50 μm hatch pattern (see Figure 6) as only one axis is well defined for the pattern. As discussed previously this is owed to the way in which the material interacts with the PMMA surface. That is, for the hatch patterns, the laser system scanned one axis first and then another giving rise to the pattern induced on the first scan being eradicated due to the melting and re-solidification arising from the second scan.

Even though the periodic hatch pattern was somewhat eradicated during the laser processing it can be seen that the surface topography was also ultimately modified in comparison to the as-received sample. It was found that the 50 μm hatch pattern gave rise to peak heights to a maximum of approximately 12 μm with the surface roughness parameters being somewhat different to the other laser patterned samples with an Sa of 3.16 μm and Ra of 0.87. This difference is born from the large difference between the Sa and Ra values for this sample. However, this can be seen to be of significance due to the fact that the Ra value could have been taken along a smoother section of the surface which had undergone melting and re-solidification. This could have resulted in a dramatic reduction of the Ra parameter. In contrast, the Sa parameter takes in to account the whole area of the continuous axonometric and as such both rougher and smoother sections of the surface would be taken in to account. Therefore, in this instance it can be argued that the Sa parameter value is more descriptive of the sample surface.

Figure 7 shows that, as a result of the laser induced hatch pattern, the surface appears smoother in comparison to the other laser patterned samples. This is owed to melting and re-solidification as the laser beam is scanned across the surface. It should also be noted that compared to Figure 6, Figure 7 shows that the 100 μm hatch pattern (H100) keeps more of the natural periodicity of the pattern owed to the fact that the larger dimensions allow for the scanned pattern to not over lap itself. The smoothness observed from the 100 μm hatch pattern (see Figure 7) was confirmed by obtaining Sa and Ra values of 1.61 and 0.98 μm, respectively. Like the 50 μm hatch pattern shown in Figure 6, the Ra parameter can be seen to be lower due to this parameter taking into account a single line profile rather than including the whole area which is incorporated in determining the Sa parameter. It was also observed that for the 100 μm hatch pattern peak heights of up to 15 μm were obtained. This result coincides with the peak height values arising from the other laser patterned samples.

4.2 – Effect of Laser Irradiation on the Wettability Characteristics

It has already been seen that the laser surface patterning has a large effect on the surface topography. As such it is highly probable that these variations in surface topography would have had a significant consequence on the resulting wettability. Table 1 shows a summary of the topography and wettability data obtained for each sample studied. In terms of wettability it can be seen that the as-received PMMA (sample AR) was predominantly hydrophilic on account of the characteristic contact angle being less than 90°. In comparison to the as-received sample (AR) there was a significant reduction in contact angle for both the 50 μm trench and hatch pattern (samples T50 and H50, respectively) allowing these samples to become more hydrophilic. In contrast, the 100 μm trench pattern (sample T100) gave rise to a contact angle that is greater than that of the as-received sample (AR) and can also be seen as hydrophobic since the contact angle is greater than 90°. It was also seen that the contact angle was equivalent to the as-received sample (AR) for the 100 μm hatch patterned sample (H100).

With regards to the 50 μm dimension patterned samples (T50 and H50) the reduction in contact angle could be seen to be a result of the increase in surface roughness, apparent polar component, γ^P, and increase in total surface energy, γ^T. This is concurrent with existing theory which states that for a hydrophilic material the contact angle should decrease upon an increase in surface roughness and apparent γ^P [4,35] Conversely, for the 100 μm trench and hatch patterned samples (T100 and H100) the contact angle was seen to increase even though the surface roughness and γ^T had increased considerably. However, for both of these samples it can be seen that γ^p decreased in comparison to the as-received sample (AR). So, it is likely, especially for sample H100, that a combination between surface roughness and γ^p was counteracting each other to obtain the observed contact angle of 84.4°, which was equivalent to the contact angle observed with AR.

One possible explanation to the observation of significant variation in contact angle for the 100 μm trench pattern (T100) is that of the dominant wetting regime present. For those samples with contact angles less than that obtained for the as-received sample (AR), it is highly likely that the Wenzel wetting regime (see Figure 8(a)) is dominant in which the whole surface wets. For the laser patterned samples which had contact angles greater than that obtained for the as-received sample it is possible that either the Cassie-Baxter regime (see Figure 8(b)) is dominant or an intermediate mixed state (see Figure 8(c)) is present. The Cassie-Baxter regime (see Figure 8(b)) describes a droplet of water on a surface which gives rise to air gaps forming along the liquid-surface boundary. Whereas the intermediate mixed state (see Figure 8(c)), as discussed by Lee and Kwon [31], refers to a droplet of liquid on a surface in which both Wenzel and Cassie-Baxter regimes are present. That is the surface roughness along with the induced pattern yields

a water droplet which is held in an intermediate state such that both wetting regimes coexist. This mixed wetting regime arising can also account for the observed reduction in apparent γ^P and increase in contact angle owed to the laser induced topographical pattern on the hydrophilic PMMA samples. This could be applied to what has been observed with the 100 μm trench pattern (T100) where the induced topographical pattern on the PMMA has given rise to the droplet sitting up on the surface giving rise to air gaps forming in the trenches of the pattern. This could then indicate that under certain circumstances the topographical pattern of the PMMA surface dominates the wettability characteristics.

In addition to the data given in Table 1, it was necessary to use XPS analysis to obtain surface chemistry data in order to detail any changes made during the laser processing. As such the data in Table 2 gives the surface composition for the as-received sample (AR), 100 μm trench sample (T100) and the 50 μm hatch sample (H50). The two laser patterned samples were decided upon by taking the samples with the greatest increase and greatest reduction in contact angle, respectively, in comparison to the as-received sample. From Table 2, it was identified that the carbon content of each of the laser patterned samples decreased slightly; whereas the oxygen content had increased slightly. It should be noted here that the other elements present arise from the manufacturing of the polymer sheets. Owing to the data given in Table 2 it is possible to determine that a change in oxygen content alone, in this instance, does not give an explanation to the variation in contact angles observed. As a result it is highly likely that the change in contact angle is dominated by a combination of the laser induced pattern, surface roughness and γ^p to give rise to different wetting regimes.

5.0 – Conclusions

This study has demonstrated that a relatively inexpensive, low power, 10W cw CO_2 laser holds the ability to significantly modify the surface of PMMA on the micron scale. With the laser powers constant (7W, 600mms^{-1}) and inducing differing patterns onto the surface it was found that the surface roughness can be increased by up to an Sa of 3 μm and an Ra of 1.6 μm in comparison to the as-received sample which yielded an Sa and Ra of 0.04 μm and 0.03 μm, respectively. It was also observed that, as a result of the thermolytical interaction between the laser beam and the material, considerable melting and re-solidification took place. In some instances, this melting and re-solidification gave rise to the eradication of the natural periodicity of the laser induced pattern. This was especially seen for the 50 μm hatch sample as the beam scan of the pattern overlapped owed to the laser spot size incident on to the material being 95 μm.

In terms of wettability it was seen that, irrespective of an increase in surface roughness and surface oxygen content, the contact angles differed over the patterns induced using the laser system. That is, for

the 50 μm dimension patterned samples a reduction in the contact angle was observed in which the samples become more hydrophilic. Whereas, the 100 μm dimension patterned samples gave rise to contact angles equivalent or greater to that of the as-received sample. For instance, the 100 μm trench pattern produced a contact angle of slightly above 90° allowing the material to become inherently hydrophobic.

There does not appear to be a clear parameter which appears to be dominating in order to explain the differing contact angles observed. However, it is possible to see that a combination of a number of parameters such as surface pattern, surface roughness and γ^p could ultimately contribute to the observed contact angle. Even so, in some instances it can be seen that a change in wetting regime owed to the surface topography could possibly be the dominating factor giving rise to contact angles larger than expected for a hydrophilic material such as nylon 6,6. As a result, one can see that more work is required to determine the contributing factors which establish the contact angle taking place.

6 – Acknowledgements

The authors would like to thank the Materials Department, Loughborough University for use of their XPS equipment. In addition, the authors would like to thank their collaborators: Directed Light Inc., East Midlands NHS Innovation Hub, Nobel Biocare and Photomachining Inc. for all of their much appreciated support. This study was financially supported by the EPSRC, (grant number EP/E046851/1).

7 – References

1. C. Mao, W. Zhao, C. Zhu, A. Zhu, J. Shen, S. Lin, In vitro studies of platelet adhesion on UV radiation-treated nylon surface, Carbohydr. Polym. 59 (2005) 19-25.

2. E. Karaca, A.S. Hockenberger, Analysis of the fracture morphology of polyamide, polyester, polypropylene, and silk sutures before and after implantation in vivo, J. Biomed. Mater. Res., Part B. 87B (2008) 580-589.

3. M. Makropoulou, A.A. Serafetinides, C.D. Skordoulis, Ultra-violet and Infra-red Laser Ablation Studies of Biocompatible Polymers, Lasers in Medical Science 10 (1995) 201-206.

4. L. Hao, J. Lawrence, Laser Surface Treatment of Bio-Implant Materials, John Wiley & Sons Inc., New Jersey, USA, 2005.

5. Y.C. Jung, B. Bhushan, Contact angle, adhesion and friction properties of micro- and nanopatterned polymers for superhydrophobicity, Nanotechnology 17 (2006) 4970-4980.

6. J. Lawrence, L. Li, Modification of the wettability characteristics of polymethyl methacrylate (PMMA) by means of CO_2, Nd:YAG, excimer and high power diode laser irradiation, Mater. Sci. Eng. A 303 (2001) 142-149.

7. J. Lai, B. Sunderland, J. Xue, S. Yan, W. Zhao, M. Folkard, B.D. Michael, Y. Wang, Study on hydrophilicity of polymer surfaces improved by plasma treatment, Appl. Surf. Sci. 252 (2006) 3375-3379.

8. F. Milde, K. Goedicke, M. Fahland, Adhesion behaviour of PVD coatings on ECR plasma and ion beam treated polymer films, Thin Solid Films 279 (1996) 169-173.

9. R.M.A. Abdul majeed, A. Datar, S.V. Bhoraskar, V. N. Bhoraskar, Surface modification of polymers by atomic oxygen using ECR plasma, Nucl. Instrum. Methods Phys. Res., Sect. B 258 (2007) 345-351.

10. S. Gollapudi, K. Samm, U. Klug, R. Kling, A. Ostendorf, Laser controlled multifunctionalization of polymer surfaces for industrial applications, in ICALEO Proceedings Laser Microprocessing Conference, LA, USA (2008) 305-312.

11. F. Yu, F. Mucklich, P. Li, H. Shen, S. Mathur, C.M. Lehr, U. Bakowsky, In vitro cell response to a polymer surface micropatterned by laser interference lithography, Biomacromolecules 6 (2005) 1160-1167.

12. F. Yu, P. Li, H. Shen, S. Mathur, C.M. Lehr, U. Bakowsky, F. Mucklich, Laser interference lithography as a new and efficient technique for micropatterning of biopolymer surface, Biomaterials 26 (2005) 2307-2312.

13. A.C. Duncan, F. Weisbuch, F. Rouais, S. Lazare, Ch. Baquey, Laser microfabricated model surfaces for controlled cell growth, Biosens. Bioelectron. 17 (2002) 413-426.

14. Z. Burton, B. Bhushan, Hydrophobicity, adhesion and friction properties of nanopatterned polymers and scale dependence for micro- and nanoelectromechanical systems, Nano Lett. 5 (2005) 1607-1613.

15. M.S. Kim, G. Khang, H.B. Lee, Gradient polymer surfaces for biomedical applications, Prog. Polym. Sci. 33 (2008) 138-164.

16. E.K.F. Yim, S.W. Pang, K.W. Leong, Synthetic nanostructures inducing differentiation of human mesenchymal stem cells into neuronal lineage, Experimental Cell Research 313 (2007) 1820-1829.

17. M.J. Dalby, D. McCloy, M. Robertson, H. Agheli, D. Sutherland, S. Affrossman, R.O.C. Oreffo, Osteoprogenitor response to semi-ordered and random topographies, Biomaterials 27 (2006) 2980-2987.

18. C.D. Skordoulis, M. Makropoulou, A.A. Serafieinides, Ablation of nylon-6,6 with UV and IR lasers. Appl. Surf. Sci. 86 (1995) 239-244.

19. E. Sarantopoulou, Z. Kollia, A.C. Cefalas, A.M. Douvas, M. Chatzichristidi, P. Argitis, S. Kobe, Polymer self-assembled nano-structures and surface relief gratings induced with laser at 157nm, Appl. Surf. Sci. 253 (2007) 7884-7889.

20. W. Pfleging, M. Bruns, A. Welle, S. Wilson, Laser-assisted modification of polystyrene surfaces for cell culture applications, Appl. Surf. Sci. 253 (2007) 9177-9184.

21. K.S Teh, Y.W. Lu, Topography and wettability control in biocompatible polymer for BioMEMs applications, in Proceedings of the 3rd IEEE Int. Conf. on Nano/Micro Engineered and Molecular Systems, Sanya, China (2008) 1100-1103.

22. Q. Zhao, C. Wang, Y. Liu, S. Wang, Bacterial adhesion on the metal-polymer composite coatings. Int. J. Adhes. Adhes. 27 (2007) 85-91.

23. E.M. Harnett, J. Alderman, T. Wood, The surface energy of various biomaterials coated with adhesion molecules used in cell culture, Colloids Surf., B 55 (2007) 90-97.

24. M. Ouhlal, R. Xu, H.P. Schreiber, Adhesion enhancement through control of acid-base interactions. J. Adhes. 80 (2004) 467-480.

25. G. Speranza, G. Gottardi, C. Pederzolli, L. Lunelli, R. Canteri, L. Pasquardini, E. Carli, A. Lui, D. Maniglio, M. Brugnara, M. Anderle, Role of chemical interactions in bacterial adhesion to polymer surfaces, Biomaterials, 25 (2004) 2029-2037.

26. X.D. Wang, X.F. Peng, J.F. Lu, T. Liu, B.X. Wang, Contact angle hysteresis on rough solid surfaces, Heat Transfer - Asian Research 33 (2004) 201-210.

27. J.T. Hirvi, T.A. Pakkanen, Wetting of nanogrooved polymer surfaces, Langmuir 23 (2007) 7724-7729.

28. Y.T Cheng, D.E. Rodak, Is the lotus leaf superhydrophobic?, Appl. Phys. Lett. 86 (2005) 144101-1-144101-3.

29. G. Whyman, E. Bormashenko, T. Stein, The rigourous derivation of young, cassie-baxter and wenzel equations and the analysis of the contact angle hysteresis phenomenon, Chem. Phys. Lett. 450 (2007) 355-359.

30. A.B.D. Cassie, S. Baxter, Wettability of porous surfaces, Trans. Faraday Soc. 40 (1944) 546-551.

31. S.M. Lee, T.H. Kwon, Effects of intrinsic hydrophobicity on wettability of polymer replicas of a superhydrophobic lotus leaf, J. Micromech. Microeng. 17 (2007) 687-692.

32. D.G. Waugh, J. Lawrence, Wettability characteristics variation of nylon 6,6 by means of CO_2 laser generated surface patterns, in ICALEO Proceedings, Pechanga, USA 101 (2008) 61-69.

33. D.G. Rance, Chapter 6 - thermodynamics of wetting: From its molecular basis to technological application, in: D.M. Brewis (Ed.), Surface Analysis and Pretreatment of Plastics and Metals, Applied Science Publishers, Essex, UK, 1982, pp.121.

34. D.G. Waugh, J. Lawrence, C.L. Thomas, D. Morgan, Interaction of CO_2 laser-modified nylon with osteoblast cells in relation to wettability., Mater. Sci. Eng., C, accepted 29th July 2009.

35. J. Lawrence, L. Li, Laser modification of the wettability characteristics of engineering materials, Professional Engineering Publishing Limited, Suffolk, UK, 2001.

36. D.G. Waugh, J. Lawrence, C.D. Walton, R.B. Zakaria, On the effects of using CO_2 and F_2 lasers to modify the wettability of a polymeric biomaterial, J. Opt. Laser Technol., accepted 5th August 2009.

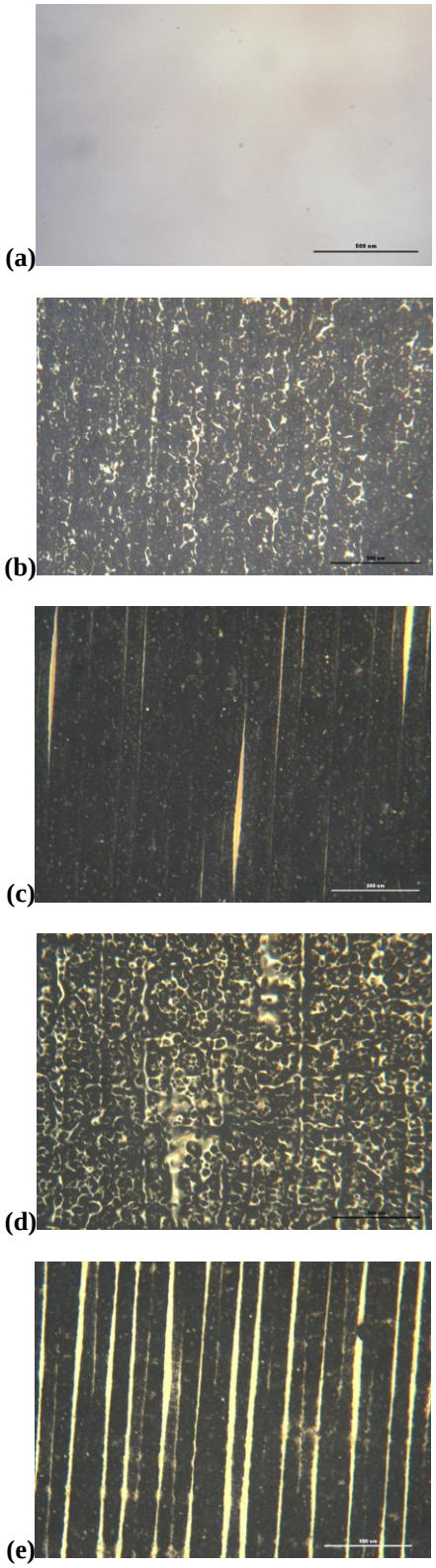

Figure 1 – Optical micrographs of PMMA samples: (a) as-received (AR), (b) 50 μm trench (T50), (c) 100 μm trench (T100), (d) 50 μm hatch (H50) and (e) 100 μm hatch (H100).

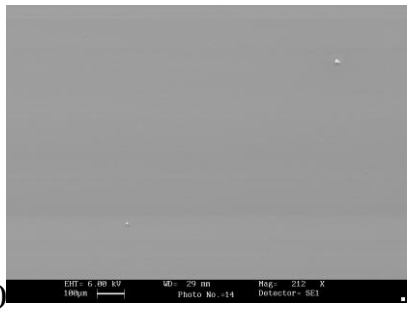

(a)

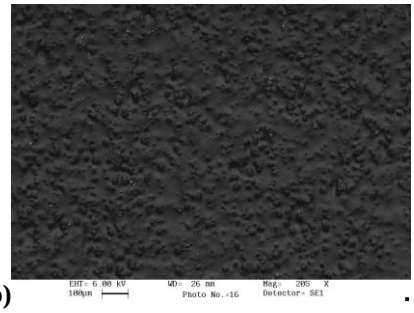

(b)

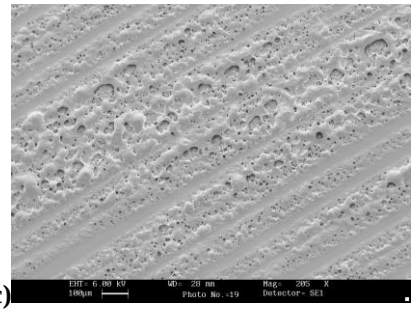

(c)

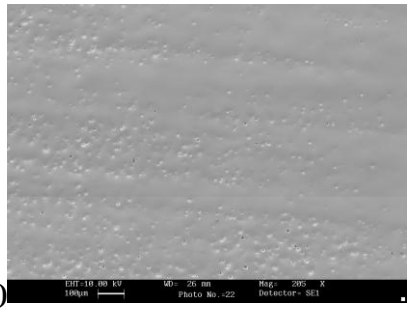

(d)

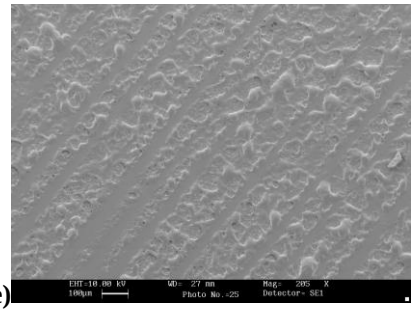

(e)

Figure 2 – SEM images of PMMA samples: (a) as-received (AR), (b) 50 µm trench (T50), (c) 100 µm trench (T100), (d) 50 µm hatch (H50), (e) 100 µm hatch (H100).

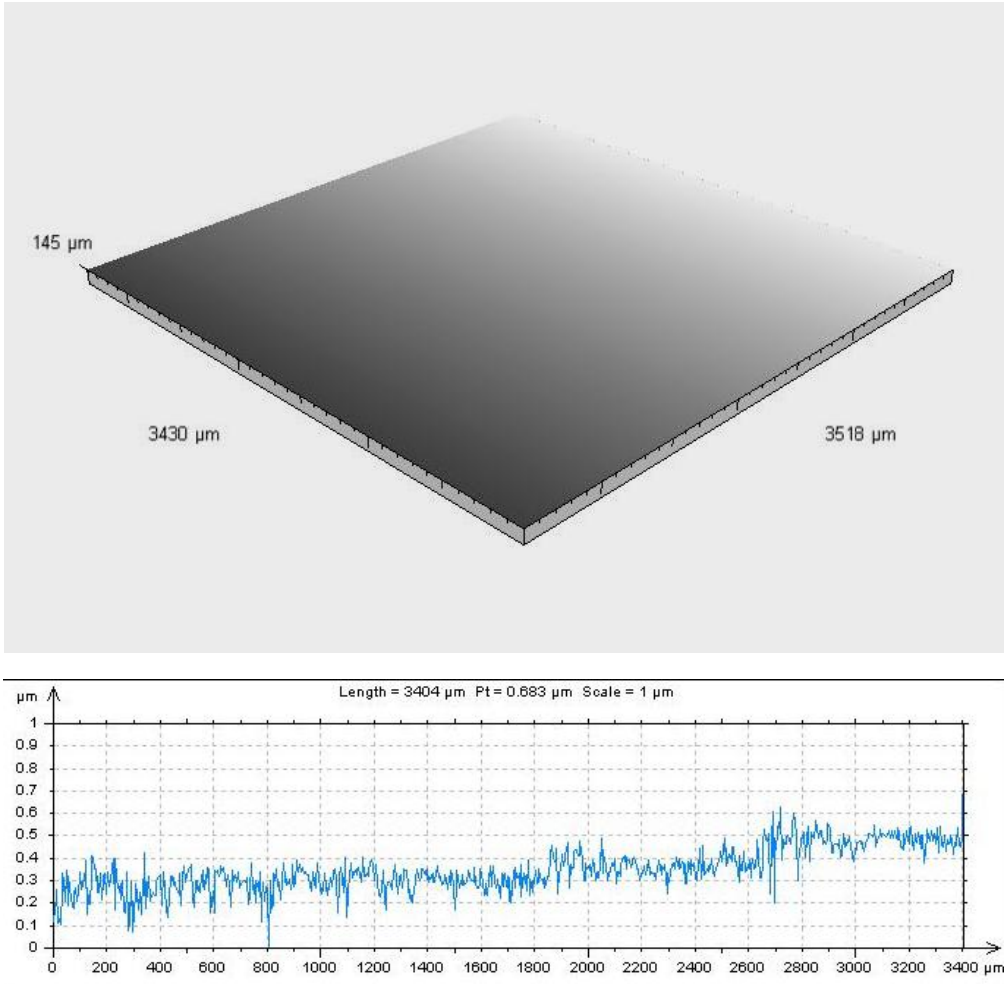

Figure 3 – Continuous axonometric and profile extraction for as-received sample (AR).

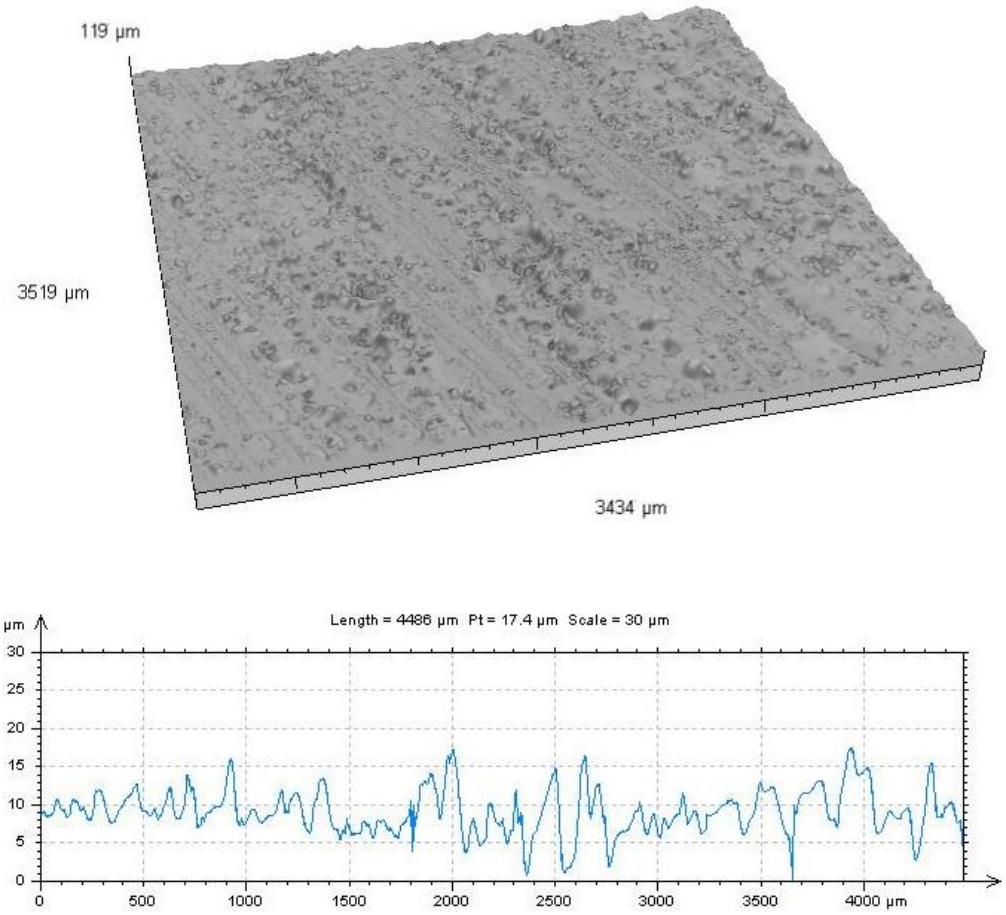

Figure 4 – Continuous axonometric and profile extraction for laser induced 50 µm trench pattern (T50).

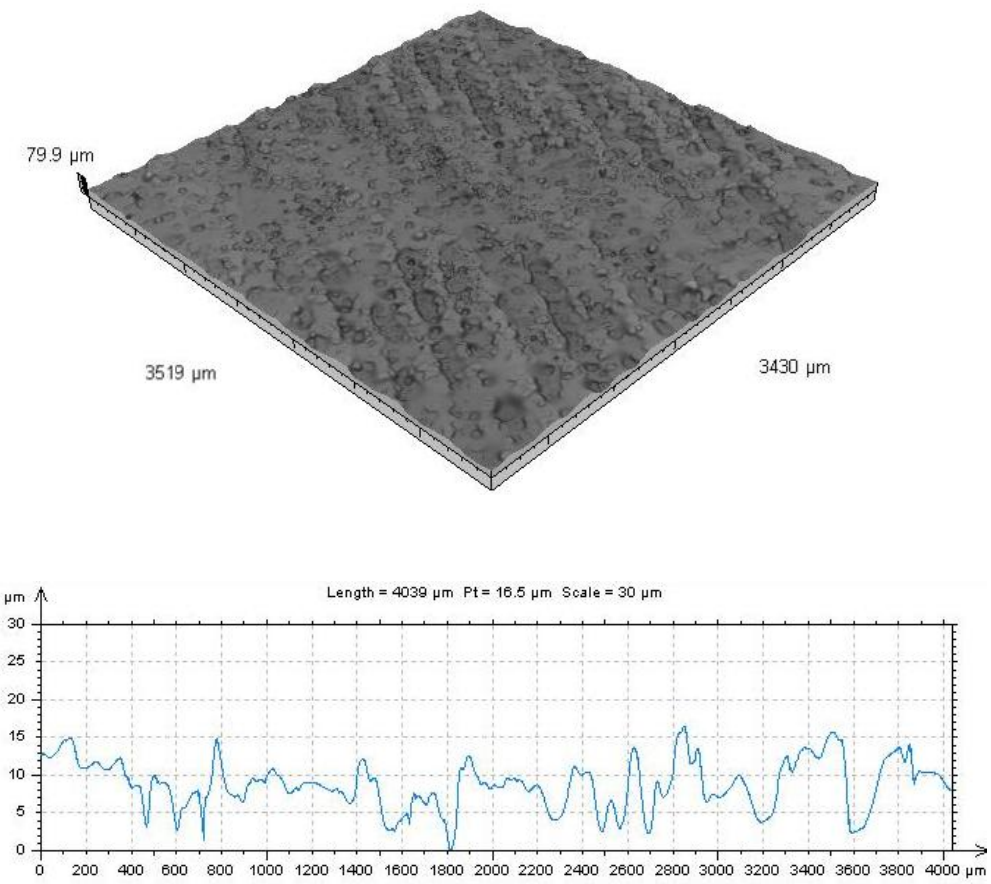

Figure 5 – Continuous axonometric and profile extraction for laser induced 100 µm trench pattern (T100).

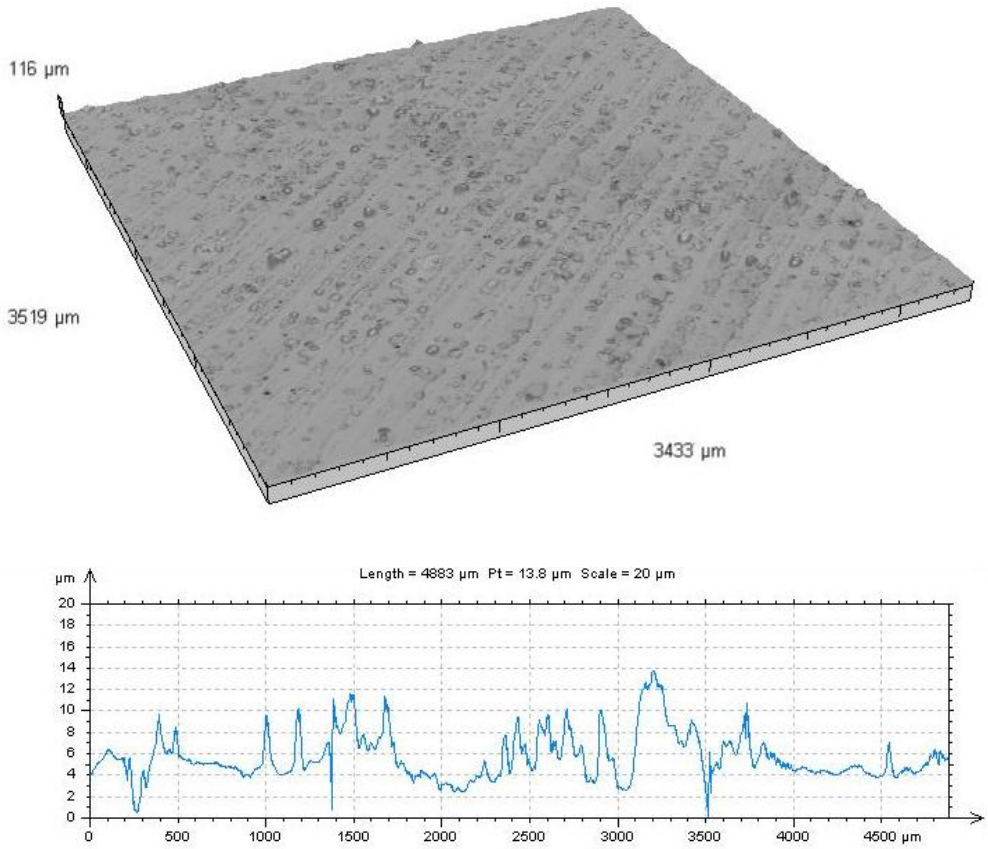

Figure 6 – Continuous axonometric and profile extraction for laser induced 50 µm hatch pattern (H50).

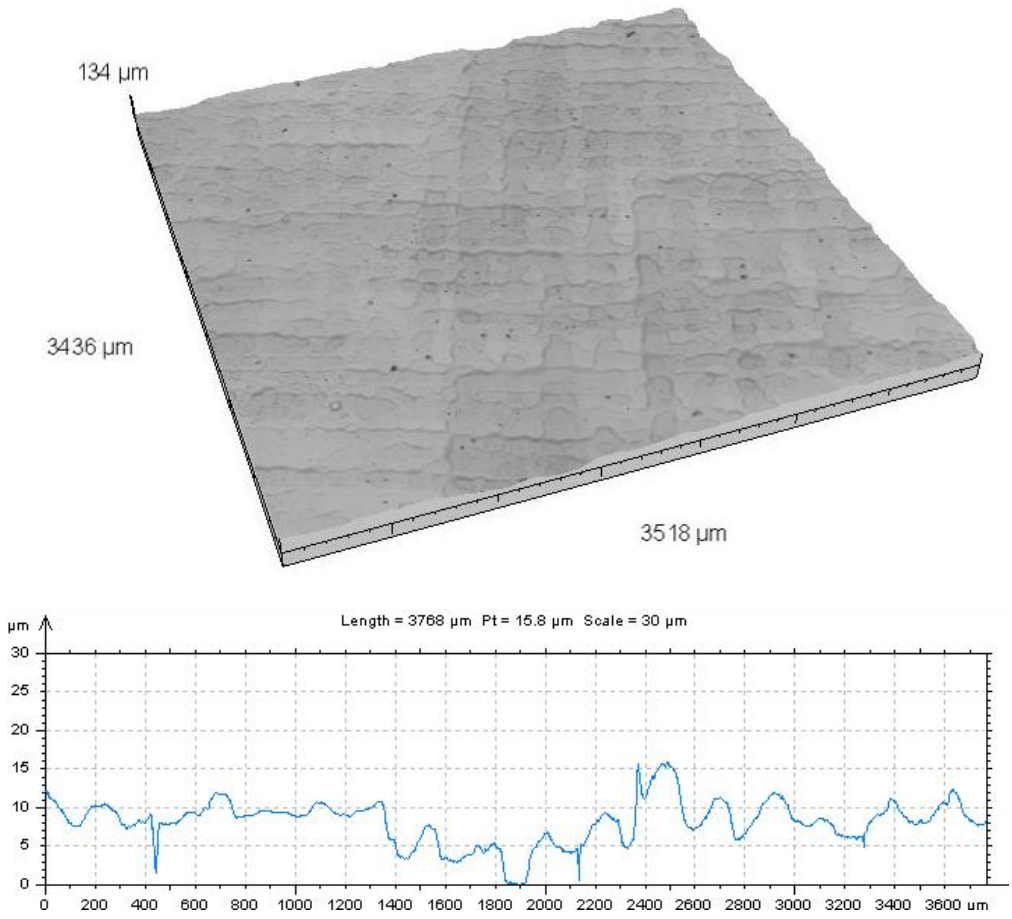

Figure 7 – Continuous axonometric and profile extraction for laser induced 100 µm hatch pattern (H100).

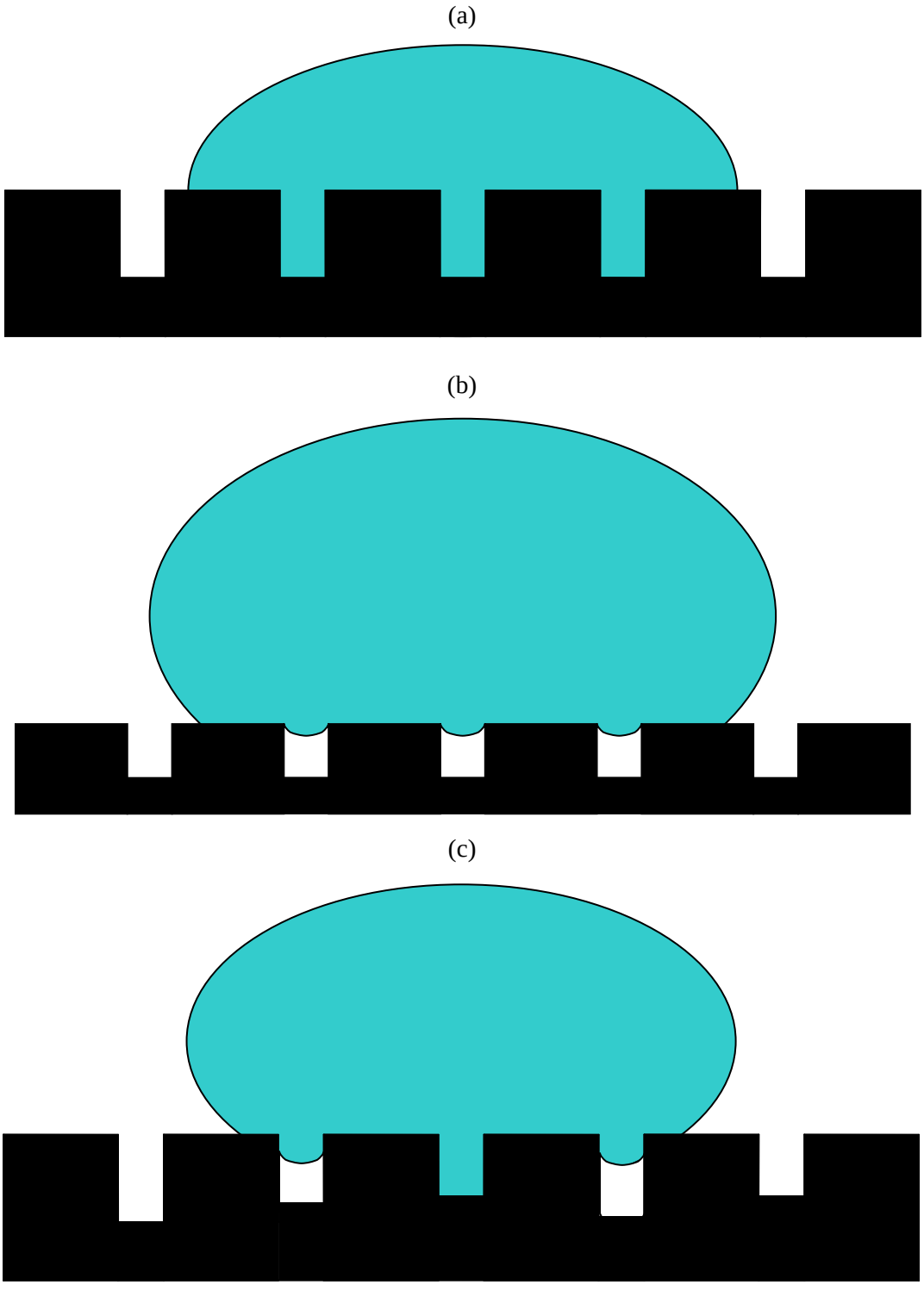

Figure 8 – Schematic diagrams showing (a) Wenzel, (b) Cassie-Baxter and (c) mixed state wetting regimes.

Table 1 – A summary of the results for the six samples along with their characteristic contact angle and hysteresis with triply distilled water.

Sample	Sa (μm)	Ra (μm)	γ^P (mJm^{-2})	γ^D (mJm^{-2})	γ^T (mJm^{-2})	Contact Angle (°)
As-Received (AR)	0.04	0.03	3.46	26.95	30.40	85.6 ±2.6
50 μm trenches (T50)	2.66	1.63	5.13	35.08	40.21	75.2 ±1.9
100 μm trenches (T100)	2.65	1.43	0.20	36.23	36.42	94.2 ±4.1
50 μm hatch (H50)	3.16	0.87	8.27	33.93	42.21	69.1 ±1.9
100 μm hatch (H100)	1.61	0.98	1.70	37.08	38.78	84.4 ±3.1

Table 2 – XPS data for selected samples.

Sample	C (% At.)	O (% At.)	N (% At.)	Si (% At.)	Na (% At.)	Cl (% At.)	S (% At.)	Zn (% At.)
As- Received (AR)	80.5	15.5	1.1	0.5	1.2	0.7	0.5	0.0
100 μm trenches (T100)	78.2	19.9	1.0	0.0	0.8	0.0	0.0	0.1
50 μm hatch (H50)	75.8	18.0	1.6	0.9	2.3	0.7	0.4	0.2